

Pion Interferometry in AuAu Collisions at $\sqrt{s_{NN}}=200$ GeV

M. López Noriega^a for the STAR Collaboration

^aThe Ohio State University, 174 W 18th Ave., Columbus, Ohio 43210, USA

We present preliminary results from a two-pion intensity interferometry analysis from Au+Au collisions at $\sqrt{s_{NN}}=200$ GeV measured in the STAR detector at RHIC. The dependence of the apparent pion source on multiplicity and transverse momentum are discussed and compared with preliminary results from d+Au and p+p collisions at the same beam energy.

1. Introduction

Two particle intensity interferometry (HBT) is a useful tool to study the space-time geometry of the particle emitting source in heavy ion collisions [1,2]. It also contains dynamical information that can be explored by studying the transverse momentum dependence of the apparent source size [3,4]. Extracted parameters in HBT analysis from Au+Au collisions at $\sqrt{s_{NN}}=130$ GeV at the Relativistic Heavy Ion Collider (RHIC) did not agree with predictions of hydrodynamic models that gave an almost perfect description of the momentum-space structure of the emitting source and elliptic flow [5]. This ‘‘HBT puzzle’’ could originate from the fact that the extracted timescales (*emission duration* from the R_o/R_s ratio and *evolution duration* from the m_T dependence of R_l) are smaller than those predicted by the hydrodynamical model [5].

In this paper we present two-pion correlation systematics as a function of the transverse total mass ($m_T = \sqrt{k_T^2 + m^2}$, $\mathbf{k}_T = \frac{1}{2}(\mathbf{p}_1 + \mathbf{p}_2)_T$) and multiplicity in Au+Au collisions at $\sqrt{s_{NN}}=200$ GeV produced by RHIC at Brookhaven National Laboratory and measured by the STAR detector. We also discuss a fitting procedure in which the strength of the final state Coulomb interaction between the two charged pions is taking into account in the fit itself.

2. Experimental Details

Experimentally, two-particle correlations are studied by constructing the correlation function $C_2(\mathbf{q}) = A(\mathbf{q})/B(\mathbf{q})$. Here $A(\mathbf{q})$ is the measured distribution of the momentum difference $\mathbf{q} = \mathbf{p}_1 - \mathbf{p}_2$ for pairs of particles from the same event, and $B(\mathbf{q})$ is the corresponding distribution for pairs of particles from different events. For this analysis we selected events with a collision vertex position within ± 25 cm measured from the center of the 4 m long STAR Time Projection Chamber (TPC), and we mixed events only if their longitudinal primary vertex positions were no farther apart than 5 cm. We divided our sample into six centrality bins, where the centrality was characterized according to the measured multiplicity of charged particles at midrapidity. The six centrality bins correspond to 0-5% (most central), 5-10%, 10-20%, 20-30%, 30-50% and 50-80% (most peripheral) of the total hadronic cross section. Charged pions were identified by correlating their specific ionization in the gas of the TPC with their measured momentum [6].

The effects of track-splitting (reconstruction of a single track as two tracks) and track-merging (two tracks with similar momenta reconstructed as a single track) were eliminated as described in [7]. A new procedure to take into account final state Coulomb interaction is described in the

next section.

The effect of the single-particle momentum resolution ($\delta p/p \sim 1\%$ for pions) induces systematic underestimation of the HBT parameters. Using an iterative procedure [7], we corrected our correlation functions for finite resolution effects. The correction due to the uncertainty on the removal of the artificial reduction of the HBT parameters associated with the anti-merging cut has been calculated in [8] and is included as systematic error.

3. Fitting procedure

The three-dimensional correlation functions were generated. The relative momentum was measured in the longitudinal co-moving system (LCMS) frame, and decomposed according to the Pratt-Bertsch [9,10] “out-side-long” parametrization. There is a Coulomb interaction between emitted particles that needs to be taken into account in order to isolate the Bose-Einstein interaction. This Coulomb interaction, repulsive for like-sign particles, causes a reduction on the number of real pairs at low q , reducing the correlation function. In our previous analysis [7,11] as well as in previous experiments, this was corrected by applying a pair Coulomb correction to each pair in the background [9] corresponding to a spherical Gaussian source of a given radius; we call this *standard* procedure. The correlation function was then fit with the functional form: $C(q_o, q_s, q_l) = \frac{A(\mathbf{q})}{B(\mathbf{q}) \times K_{coul}(q_{inv})} = 1 + \lambda \exp(-R_o^2 q_o^2 - R_s^2 q_s^2 - R_l^2 q_l^2)$, where $K_{coul}(q_{inv})$ is the square of the Coulomb wave-function. However, this procedure overcorrects the correlation function since all background pairs are corrected, including those that are not formed by primary pions.

We have implemented a new procedure, first suggested by Bowler [12] and Sinyukov [13] and recently used by the CERES collaboration [14], in which the strength of the Coulomb interaction is taken into account in the fit itself and only pairs with Bose-Einstein interaction are considered to Coulomb interact; we call this *Bowler-Sinyukov* procedure. The fit in this case is: $C(q_o, q_s, q_l) = \frac{A(\mathbf{q})}{B(\mathbf{q})} = (1-\lambda) + \lambda K_{coul}(q_{inv})(1 + \exp(-R_o^2 q_o^2 - R_s^2 q_s^2 - R_l^2 q_l^2))$, where $K_{coul}(q_{inv})$ is the same as above.

In Figure 1, the measured $\pi^+\pi^-$ correlation function is compared to several calculations. Lines indicate the *standard* ($K_{coul}(Q_{inv})$) and *Bowler-Sinyukov* ($(1 + (\lambda - 1)K_{coul}(Q_{inv}))$) Coulomb functions; in the latter, λ was extracted from the fit to the 3D like-sign correlation function. Clearly, the *Bowler-Sinyukov* function better reproduces the data. Further improvement is observed when the strong interaction (negligible for like-sign pion correlations) is included [15] into the $\pi^+\pi^-$ final state interactions.

When we use this procedure in our 3D analysis we observe an increase in R_o of 10-15%. The values of R_s and R_l do not depend significantly on the Coulomb procedure. Consequently the increase in R_o/R_s is not enough to solve the HBT puzzle.

4. HBT parameters versus centrality and transverse momentum

Figure 2 shows the m_T dependence of the source parameters for pions at six centrality bins from Au+Au collisions as well as from p+p and d+Au collisions at same beam energy. The three radii increase with increasing centrality and R_l varies similar to R_o and R_s ; for R_o and R_s this increase may be attributed to the geometrical overlap of the two nuclei. The extracted radii rapidly decrease as a function of m_T , which is an indication of transverse flow [16]. In order to extract information about the m_T dependence on centrality, we fit the m_T dependence of each radius and each centrality to a power-law function: $R_i(m_T) = R_{i0} \cdot m_T^{-\alpha}$ (solid lines in Figure 2). Figure 3 shows the dependence of α on the number of participants; for Au+Au, α is constant for R_l as a function of number of participants and decreases with the number of

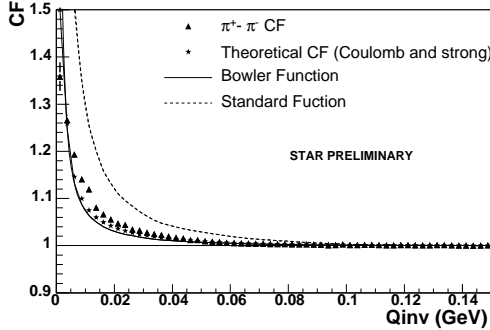


Figure 1. Experimental (triangles) and theoretical [15] (stars) 1D $\pi^+\pi^-$ correlation functions compared with *standard* (dotted line) and *Bowler-Sinyukov* (continuous line) functions.

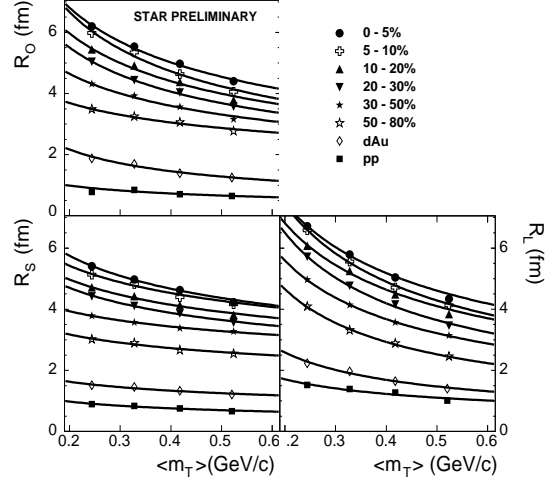


Figure 2. HBT radii for 6 different centrality from Au+Au collisions, and from p+p and d+Au collisions. The lines indicate power-law fits to each parameter and centrality.

participants for R_o and R_s for the most peripheral bins indicating a decrease of transverse flow for these collisions. $R_o/R_s \sim 1$ which indicates a short emission duration in a blast wave fit [17].

Assuming boost-invariant longitudinal flow we can extract an evolution time-scale by using a simple fit [17]: $R_l = \langle t_{fo} \rangle \sqrt{\frac{T}{m_T} \frac{K_2(m_T/T)}{K_1(m_T/T)}}$ where T is the freeze-out temperature and K_1 and K_2 are the modified Bessel functions of order 1 and 2. For T extracted from fits to pion, kaon, and proton transverse momentum spectra (90 MeV for most central and 120 MeV for most peripheral collisions) [18] we get $\langle t_{fo} \rangle \approx 9$ fm/c for central events and $\langle t_{fo} \rangle \approx 6$ fm/c for peripheral events. Hence, the evolution time, in addition to the emission duration, is quite short.

For a transverse expanding, longitudinally boost-invariant source, and assuming a Gaussian transverse density profile, we can extract information about its radius, R_{geom} , by fitting the m_T dependence of R_s to: $R_s(m_T) = \sqrt{\frac{R_{geom}^2}{1 + \eta_f^2 (\frac{1}{2} + \frac{m_T}{T})}}$ where T is again the freeze-out temperature and η_f is the surface transverse rapidity [19]. For T and η_f consistent with spectra we see an increase on this radius from ~ 5 fm for the most peripheral case to ~ 13 fm for the most central one as shown in Figure 4. We also observe a smooth transition from p+p ($N_{participants} = 2$) and d+Au ($N_{participants} = 8.3$) to Au+Au collisions.

5. Conclusion

We have presented identical pion interferometry results for Au+Au collisions at $\sqrt{s_{NN}}=200$ GeV. With respect to multiplicity and m_T dependencies, pion HBT radii are very similar to results reported at $\sqrt{s_{NN}}=130$ GeV. HBT radii and geometrical radius increase with increasing

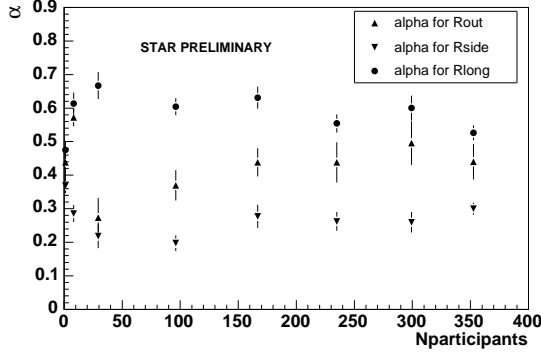


Figure 3. Extracted α parameter from the power-law fits to the HBT radii (lines in Figure 2) for p+p, d+Au and 6 different centralities in Au+Au collisions

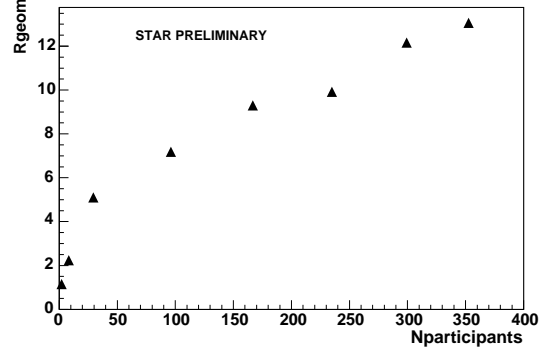


Figure 4. Extracted R_{geom} radius for a transverse gaussian density profile [19] for p+p, d+Au and 6 different centralities in Au+Au collisions

centrality. HBT radii decrease with m_T and we observe a stronger flow for the most central collisions. Our results indicate that both the evolution timescale (as measured by the m_T dependence of R_l) and the emission duration (probed by comparing R_o to R_s) are surprisingly fast. The Bowler-Sinyukov Coulomb procedure does not solve the “HBT puzzle” although increases the ratio R_o/R_s by 10-15%.

REFERENCES

1. W. Bauer, C.K. Gelbke and S. Pratt, Annu. Rev. Nucl. Part. Sci. **42**, 77 (1992).
2. U. Heinz and B. Jacak, Annu. Rev. Nucl. Part. Sci. **49**, 529 (1999).
3. S. Pratt, Phys. Rev. Lett. **53**, 1219 (1984).
4. A.N. Makhlin and Y.M. Sinyukov, Z. Physics. C **39**, 29 (1988).
5. U. Heinz and P. Kolb, hep-ph/0204061.
6. K. H. Ackermann *et al.* (STAR Collaboration), Nucl. Instrum. Meth. **A499**, 624 (2003).
7. C. Adler *et al.* (STAR Collaboration), Phys. Rev. Letter. **87**, 082301 (2001).
8. J. Adams *et al.* (STAR Collaboration), submitted to Phys. Rev. Lett.; nucl-ex/0312009.
9. S. Pratt, T. Csörgö, and J. Zimanyi, Phys. Rev. C **42**, 2646 (1990).
10. G. Bertsch, Nucl. Phys. **A498**, 173c (1989).
11. M. López Noriega for the STAR Collaboration, Nucl. Phys. **A715**, 623c (2003).
12. M. G. Bowler, Phys. Lett. B **270**, 69 (1991)
13. Yu. M. Sinyukov *et al.*, Phys. Lett. B **432**, 249 (1998).
14. D. Adamova *et al.* (CERES Collaboration), Nucl. Phys. A **714**, 124 (2003).
15. R. Lednicky and V. L. Lyuboshitz, Yad. Fiz **35**, 1316 (1982) [Sov. J. Nucl. Phys. **35**, 770 (1982)]. Fortran program provided by R. Lednicky.
16. B. Tomasik *et al.*, Nucl. Phys. **A663**, 753(2000).
17. F. Retière and M. A. Lisa, nucl-th/0312024.
18. J. Adams *et al.* (STAR Collaboration), submitted to Phys. Rev. Lett.; nucl-ex/0310004
19. U. Wiedemann, P. Scotto and U. Heinz, Phys. Rev. **C53**, 918 (1996)